

ROLE OF Sr DOPANTS IN THE INHOMOGENEOUS GROUND STATE OF $\text{La}_{2-x}\text{Sr}_x\text{CuO}_4$

D. HASKEL¹, E. A. STERN² and F. DOGAN³

¹Experimental Facilities Division, Advanced Photon Source
Argonne National Laboratory, Argonne, IL 60439, USA

²Department of Physics, University of Washington
Seattle, WA 98195-1560, USA

³Department of Materials Science and Engineering, University of Washington
Seattle, WA 98195-2120, USA

INTRODUCTION

The role of dopants in high T_c superconductors is widely seen as being limited to the introduction of hole carriers into the CuO_2 planes of otherwise insulating parent compounds. This simplified assumption is partly driven by the lack of information on the local atomic and electronic structure around dopants. While experimental evidence favoring inhomogeneous charge distributions of the doped holes is still mounting, the role that dopants play in determining this inhomogeneous ground state, if any, is still unclear. Since high T_c superconductors manifest strong carrier-lattice interactions, as evidenced, e.g., in the presence of *Jahn-Teller* distorted CuO_6 octahedra, structural techniques can, in principle, provide information on the spatial distribution of doped charges through the structural response. The x-ray absorption fine structure (XAFS) technique is particularly suited for elucidating such response around dopants, as it is element specific; i.e., by tuning the x-ray energy to a characteristic absorption threshold of a given dopant, it can determine the *partial* pair correlations between the dopant and its neighbors. This is of paramount importance since the dopants substitute at the crystal sites of the majority atoms and therefore techniques that sum over all pair correlations are dominated by the correlations involving the majority, host, atoms. In this paper we present evidence that the doped holes are spatially correlated to Sr dopants in $\text{La}_{2-x}\text{Sr}_x\text{CuO}_4$. This is manifested as a unique structural response of the Sr-O(2) distance across the $x \sim 0.06$ insulator-metal transition, while no such response is observed for the La-O(2) distance. This result by itself proves that the doped charge density is not uniformly distributed, and that the dopants play a role in determining the inhomogeneous charge state. In addition to local effects around dopants, we show evidence for the appearance, with Sr

doping, of an inhomogeneous *structural* ground state at $x \gtrsim 0.15$. This ground state is characterized by the presence of local domains with a larger orthorhombic distortion than the long-range averaged distortion determined by crystallography.

EXPERIMENTAL

Samples of $\text{La}_{2-x}\text{Sr}_x\text{CuO}_4$ were prepared by (i) conventional solid-state reaction techniques starting from related oxides (Radaelli *et al.* [1], $0.07 \leq x \leq 0.36$) and (ii) by precipitation from ionic solution starting from related nitrates (Haskel *et al.* [2], $0 \leq x \leq 0.15$). T_c 's were determined by magnetic susceptibility measurements and average crystal structures were determined by neutron and x-ray powder diffraction (Refs. 1 and 2). The local environment around La/Sr atoms in $\text{La}_{2-x}\text{Sr}_x\text{CuO}_4$ is quite complex and includes nine oxygen neighbors at six different distances. In a powder XAFS experiment, an angular-average over all the relative orientations of the electric field vector and the La/Sr-O bond directions is performed. There is simply not enough information in a powder XAFS experiment to resolve all the different distances. By performing our experiments on *c*-axis magnetically aligned powders, we can exploit the angular dependence of the XAFS signal in the anisotropic (layered) cuprates to measure subsets of the local structure around the absorbing atom allowing a complete determination of the local structure. (For excitation of a $1s$ core electron, i.e., *K*-edges, this dependence is a $\cos^2\theta$ one, with θ the angle between the electric field vector and the bond orientation). Since we are particularly interested in structural ground state properties, we present here results of measurements performed at $T=10\text{K}$ using a closed cycle helium dilution refrigerator. Orientation-dependent spectra were taken by rotating the oriented samples relative to the electric field vector of the synchrotron radiation. Experiments were performed at the National Synchrotron Light Source (NSLS, Brookhaven) and at the Advanced Photon Source (APS, Argonne). La *K*-edge measurements were performed in transmission geometry, which determines the energy-dependent absorption coefficient by measuring the attenuation of the x-ray intensity after passing through the sample thickness. Sr *K*-edge measurements were done in both transmission ($x \geq 0.04$) and fluorescence ($x \leq 0.04$) geometries, where the latter determines the absorption coefficient by measuring the secondary radiation that accompanies the de-excitation of the absorbing atom. The reader is referred to Refs. 1-3 for further experimental details.

RESULTS

Figure 1 shows local Sr-O(2) and La-O(2) apical distances as determined from *c*-axis polarized XAFS experiments at Sr and La *K*-edges as a function of Sr content in $\text{La}_{2-x}\text{Sr}_x\text{CuO}_4$ at $T=10\text{K}$. The O(2) oxygens form the apices of CuO_6 octahedra and the La/Sr-O(2) apical bonds nearly coincide with the crystallographic *c*-axis (slightly off *c*-axis due to $\approx 3^\circ$ tilts of CuO_6 octahedra and correlated off-center displacements of La/Sr atoms in the La_2O_2 planes. See Radaelli *et al.*[1] for a detailed description of the crystal structure). We have previously reported evidence for the existence of a double site distribution for the apical O(2) oxygens only near Sr atoms, a distribution that can be described as two Sr-O(2) distances at $r \approx 2.25, 2.55 \text{ \AA}$, respectively, with relative weights that strongly depend on x (Haskel *et al.*[4]). These previous results were obtained on samples prepared by solid-state reaction. The samples prepared by precipitation from solution did not show the broad (split) distribution in the Sr-O(2) distance, indicating a more homogeneous Sr environment in the latter. Since samples from both families have similar values of T_c , it is implied that the double site distribution observed previously must not be related to the mechanism of superconductivity.

The single Sr-O(2) distance found in the samples precipitated from solution, however,

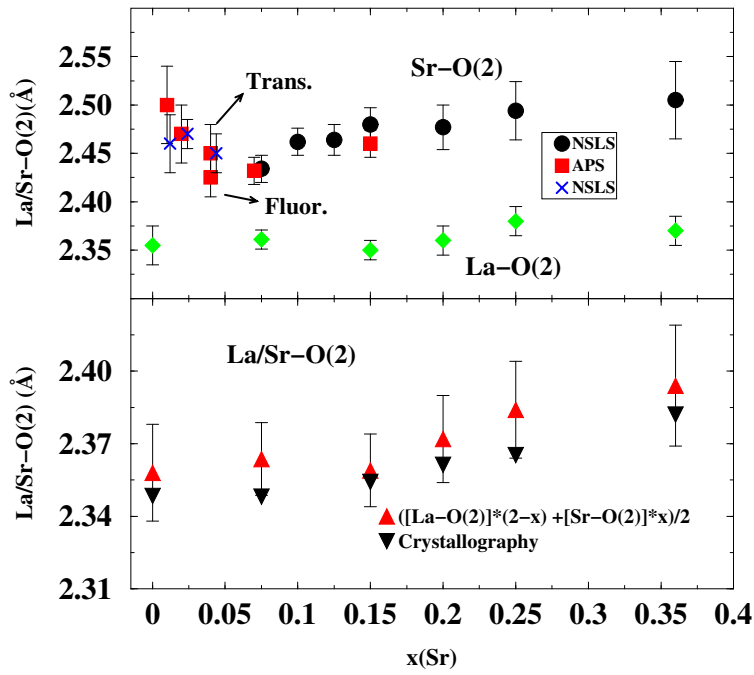


Figure 1. Top: Local Sr-O(2) (centroids) and La-O(2) apical distances obtained from c -axis polarized Sr and La XAFS at their K -edges at $T=10\text{K}$. Sr measurements were done on samples prepared by solid state reaction (circles) and by precipitation from solution (squares, crosses) and at different synchrotron facilities (APS, NSLS). Results from both transmission and fluorescence measurements are shown for comparison for $x = 0.04$. Crosses are displaced in x for clarity. Bottom: weighted averages of Sr-O(2) and La-O(2) distances as a function of x and their comparison with the results of crystallography.

agrees well with the weighted average of the two Sr-O(2) distances found previously. This is shown in Fig. 1 where the *centroid* of the Sr-O(2) apical distribution is plotted for samples made by the different methods ($x = 0.07, 0.15$). Good agreement is also obtained for Sr-O(2) distances obtained by measuring XAFS at the Sr K -edge in transmission and fluorescence geometries ($x = 0.04$) as well as between measurements performed at different synchrotron facilities ($x \leq 0.04$).

Figure 1 shows that the *local* Sr-O(2) apical distance is significantly longer than the *local* La-O(2) distance. Their weighted average, $([\text{La-O}(2)]*(2-x) + [\text{Sr-O}(2)]*x)/2$, agrees with the values obtained by crystallography, as expected (lower panel of Fig. 1). The longer Sr-O(2) local distance is readily explained by the stronger attraction of a negatively charged O(2) ion to a trivalent La^{+3} ion than to a divalent Sr^{+2} . This has significant implications for the local electronic structure of $\text{La}_{2-x}\text{Sr}_x\text{CuO}_4$, as discussed below. The local La-O(2) distance is nearly independent of x , and therefore the average expansion of the La/Sr-O(2) distance determined by crystallography as the Sr content is increased is due to the increase in weight, with x , of the long Sr-O(2) distance. A more striking observation is the change in slope that is observed *only* in the Sr-O(2) distance at $x \sim 0.06$ but *not* in the La-O(2) distance. We recall that in $\text{La}_{2-x}\text{Sr}_x\text{CuO}_4$ an insulator-metal (I-M) transition takes place at $x \approx 0.06$. The response of the Sr-O(2) distance to the delocalization of doped holes is indicative of a spatial correlation between these doped holes and the Sr dopants. This observed change in slope explains a similar (but opposite) change in slope measured by crystallography in the x dependence of the Cu-O(2) apical distance (Figure 2 and Ref. [1]). O(2) apicals bridge Cu and La/Sr atoms in a nearly collinear configuration. Since we know from Sr and La XAFS that the Sr-Cu and La-Cu distances along the c -axis are nearly identical (within 0.01\AA , Haskel *et al.* [5]) the Cu-O(2) apical distance measured by diffraction is a weighted average of a majority long Cu-O(2) distance (near La) and a minority short Cu-O(2) distance (near Sr),

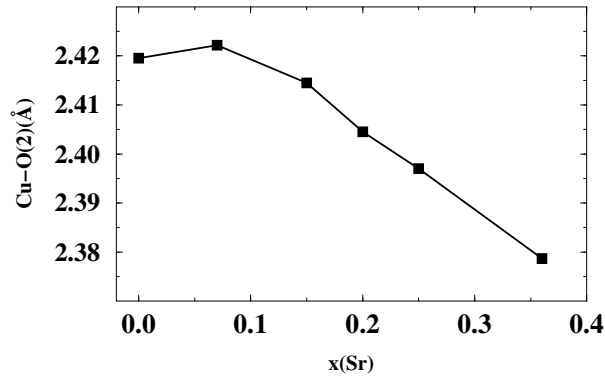


Figure 2. Cu-O(2) apical distance measured by crystallography (Radaelli *et al.*[1]). The change in slope at the I-M transition reflects the similar (but opposite in sign) change in slope observed in the Sr-O(2) apical distance.

with the latter showing a reversal in slope at the I-M transition.

We now turn to the experimental evidence showing the appearance of nanodomain structure in $\text{La}_{2-x}\text{Sr}_x\text{CuO}_4$ for $x \geq 0.15$. The structural phase diagram of $\text{La}_{2-x}\text{Sr}_x\text{CuO}_4$ indicates a low temperature orthorhombic (LTO) ground state with correlated CuO_6 octahedral tilts of magnitude $\sim 3^\circ$ about $\langle 100 \rangle$ crystallographic axis. Crystallography finds that as the Sr content is increased the tilt angle of CuO_6 octahedra gradually decreases, becoming zero at $x \sim 0.21$ (at $T=10\text{K}$), at which point the second-order phase transition to a macroscopically tetragonal phase (HTT) is completed. Figure 3 shows the different tilt patterns of CuO_6 octahedra encountered in La-cuprates. The Sr-doped system only exhibits the LTO and HTT phases, as determined by neutron diffraction. It is immediately obvious from Fig. 3 that by measuring Cu-O(1) and Cu-O(2) distances (i.e. the Cu atoms nearest neighbors' distances) it is not possible to determine the *direction* nor the *magnitude* of the CuO_6 octahedra tilts. This is because the tilts are nearly rigid and their magnitude too small to produce any measurable changes in the near-neighbors distances within the sensitivity of XAFS, $\sim 0.01 \text{ \AA}$. The O(2) apical atoms lie in the La_2O_2 planes and different tilt directions and/or magnitudes result in significantly different La-O(2) planar radial distribution functions (Figure 3). Therefore by measuring in-plane polarized XAFS *at the La site*, we are extremely sensitive to tilt direction and magnitude. By measuring the local La-O(2) planar distribution of distances as a function of x we can follow the structural phase transition from the LTO phase (3 distances) to the HTT phase (a single distance).

Figure 4 shows the results of such measurements. It is immediately obvious that although the local splitting (and therefore the local magnitude of tilt angle) initially decreases up to $x \sim 0.15$, the local splitting deviates from the macroscopic value determined by crystallography above this concentration. In particular, whereas the averaged tilt angle goes to zero at the LTO \rightarrow HTT phase transition ($x = 0.21$), the local tilts do not vanish.

DISCUSSION

That the Sr-O(2) distance shows a large response to the delocalization of holes at the I-M transition but the La-O(2) distance does not (Figure 1) is direct evidence that a spatial correlation exists between the doped holes and the dopants that introduced them. This might not be surprising, as at low Sr concentrations the dopants' potential is poorly screened and it is energetically favorable for a doped hole to remain in the vicinity of the Sr. At larger dopant concentrations screening becomes more efficient but remains poor at very short distances, so the doped holes, even if itinerant, are expected to have significant weight in the vicinity of

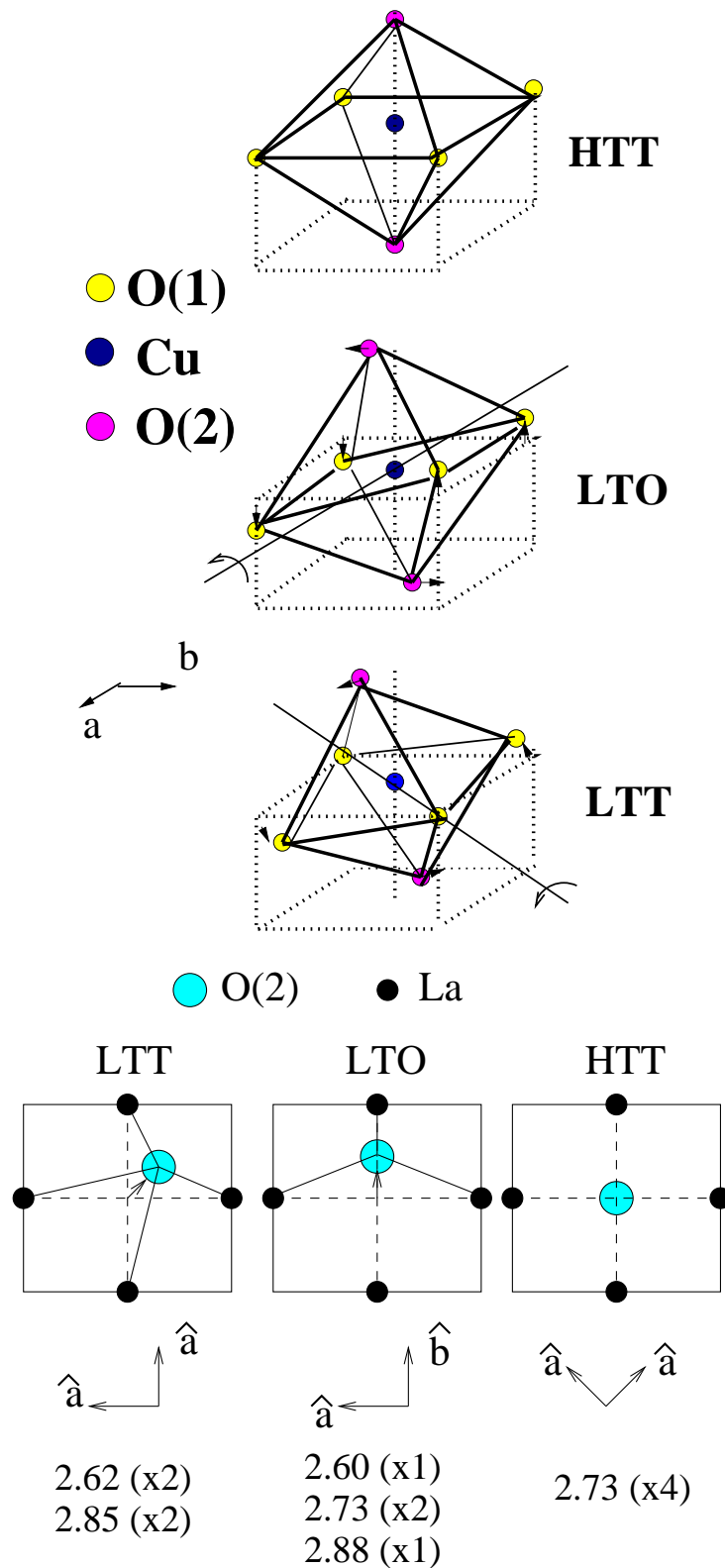


Figure 3. Top: The different CuO₆ octahedral tilt patterns encountered in La-cuprates together with the resultant La-O(2) planar distances caused by such tilts. Crystallography finds that only the LTO and HTT phases materialize in La_{2-x}Sr_xCuO₄. While XAFS at the Cu sites is nearly insensitive to tilt direction and magnitude, XAFS at the La sites is very sensitive to both as seen in the very different radial distribution functions of La-O(2) distances. The splitting in La-O(2) distances is directly proportional to the magnitude of octahedral tilts.

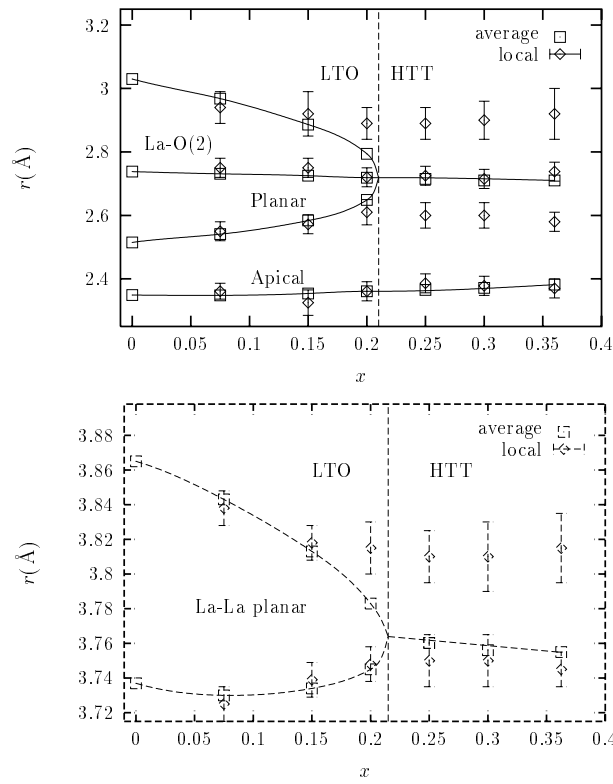


Figure 4. La-O(2) planar and La-La planar distances as a function of x determined by in-plane (electric field parallel to La_2O_2 planes) polarized La K -edge XAFS in $\text{La}_{2-x}\text{Sr}_x\text{CuO}_4$ at $T=10\text{K}$. Solid lines show the results of crystallography (Radaelli *et al.*[1]), with the macroscopically averaged splitting of La-O(2) and La-La planar distances going to zero at $x = 0.21$ (the splitting is proportional to the tilt angle of CuO_6 octahedra). The XAFS results show that, although decreasing up to $x = 0.15$, the splitting remains present in the local structure (as do the tilts) even in the nominal HTT phase.

the dopants. The structural response to the change in localization of the holes also shows that there is a strong local interaction between the doped hole and the lattice. We believe this is the first direct experimental evidence for a spatial correlation between dopants and doped holes, although a similar conclusion was derived from the interpretation of NQR data by Hammel *et al.*[6].

The local distortion in the Sr-O(2) apical distance has an important role in determining the local electronic structure of La-cuprates. The electronic orbital character of doped holes was determined by polarization-dependent x-ray absorption near edge structure (XANES) measurements, which, at the absorption threshold, determine the density of unoccupied states (holes) at the Fermi level, projected into the angular momentum states allowed by dipole selection rules. O K -edge (1s) measurements showed that doped holes acquire more out-of-plane, O $2p_z$ orbital character, compared to their in-plane, O $2p_{x,y}$ character, as doping is increased (Chen *et al.*[7]). This phenomenon is hard to explain by band structure calculations using the periodic average structure of crystallography and a rigid band model to account for the changes in chemical potential with doping. However, the introduction of Sr^{+2} dopants results in a long, local, Sr-O(2) distance which raises the local energy of O $2p_z$ orbitals towards the Fermi level, allowing them to become more populated by the doped holes. The raise in orbital energy is due to both a smaller Madelung energy contribution of the Sr^{+2} ions compared to La^{+3} together with an increased overlap of O $2p_z$ orbitals with Cu $3d_{3z^2-r^2}$ ones that results from the closer O(2)-Cu distance. The XANES measurement cannot determine *which* oxygens in the structure are being populated by the doped holes, as it averages over all oxygens. Our measurements indicate that the out-of-plane holes are being introduced in O(2) apicals neighboring the Sr dopant atoms.

This result is crucial in understanding the c -axis transport properties of $\text{La}_{2-x}\text{Sr}_x\text{CuO}_4$, as O $2p_z$ orbitals provide connectivity along the c -axis. For example, the c -axis normal state conductivity is insulating/semiconducting throughout the superconducting region of the phase diagram, due to the small overlap of O $2p_z$ orbitals (the normal state ab -plane conductivity is metallic). As the Sr content increases, this overlap increases with a concomitant increase in c -axis conductivity, to result in c -axis metallic conduction at $x \sim 0.25$. (At this concentration of dopants, ca. 12% of La sites, a random distribution of Sr atoms results in at least two Sr atoms per unit cell).

That the structure of $\text{La}_{2-x}\text{Sr}_x\text{CuO}_4$ is composed of nanodomains for $x \geq 0.15$ is readily seen from Figure 4. For these concentrations the local structure is different from the average structure; specifically the local tilt angle of CuO_6 octahedra (and the related splitting of La-O(2) and La-La planar distances) is larger than its macroscopically averaged value. In particular, while the long range averaged tilt becomes zero at $x \sim 0.21$, the local tilt remains, with a magnitude of comparable size to the one at $x = 0.15$. This can be explained by the presence of structural disorder in the form of nanodomains. XAFS obtains local structural information within a length scale that is determined by the photoelectron mean free path, $\sim 10\text{\AA}$. Diffraction techniques average over much longer length scales. In order for the macroscopically averaged tilt angle to be smaller than the local tilt the latter has to become disordered over the length scale measured by diffraction. The tilts, therefore, are locally ordered within domains whose size is determined by the correlation length of this ordering. These domains are at least as big as the XAFS length scale ($\sim 10\text{\AA}$) as no evidence for local disorder is found in the XAFS measurements. We do not see the domain boundaries in our measurements but we can put an upper limit, on the order of 50\AA , to the domain size. Larger LTO domains would be visible in the diffraction measurements, but those were not observed. The presence of nanodomains with size l , $10 \lesssim l \lesssim 50\text{\AA}$, for $x \geq 0.15$ is a direct consequence of our measurements.

Most theories aiming at describing the transport properties of $\text{La}_{2-x}\text{Sr}_x\text{CuO}_4$ limit the Sr dopants' involvement to their introduction of hole carriers into the CuO_2 planes. A much more active role for the dopant sites is postulated by J. C. Phillips in the context of his zigzag filamentary theory of high T_c superconductors (Phillips [8]). In this theory dopants are resonant tunneling centers that serve the role of providing interlayer connectivity by creating a percolative current path. A large carrier-lattice coupling at the dopant sites aids in establishing this connectivity. The observation, in our measurements, of a structural response in the Sr environment (and not in the La one) to hole-delocalization at the I-M transition is a signature of the inhomogeneity of the wave function of the doped holes, which is peaked in the vicinity of the dopant sites. This provides some support for the ideas in Ref. [8] which also depend on the inhomogeneity of the carriers' wave function and on a large hole-lattice coupling at the dopant sites.

The appearance of structural disorder at $x \geq 0.15$ could be related to the decrease of T_c in the overdoped regime; however, it has also been argued that the presence of local, short-ranged orthorhombic domains with orthorhombic distortion larger than the macroscopic orthorhombic distortion measured by crystallography favors superconductivity (Phillips [8]). The role played by disorder introduced with dopants is currently being debated, particularly how it influences the topology of inhomogeneous charge distributions in high T_c cuprates (Hasselmann *et al.*[9]).

Summary

Our experiments in $\text{La}_{2-x}\text{Sr}_x\text{CuO}_4$ provide evidence for a spatial correlation between the doped holes and the Sr dopants, in addition to the presence of a large hole-lattice coupling *only* in the vicinity of the Sr dopants. The local structure deviates from the macroscopic, average, structure at $x \geq 0.15$, indicating the appearance of structural disorder. This disorder is in

the form of nanodomains, within which the local tilts are ordered, but tilts become disordered relative to each other in going from one domain to the other. These results indicate that Sr dopants might have a much more significant role in determining normal and superconducting properties of $\text{La}_{2-x}\text{Sr}_x\text{CuO}_4$ than is typically assumed.

Acknowledgments

It is a pleasure to thank V. Polinger, J. C. Phillips, Y. Yacoby, A. R. Moodenbaugh, D. G. Hinks, A. W. Mitchell, J. D. Jorgensen, F. Perez and M. Suenaga for valuable discussions. This work supported by DOE grant no. DE-FG03-98ER45681 and DOE contract no. W-31-109-Eng-38.

REFERENCES

1. Radaelli, P.G., Hinks, D. G., Mitchell, A.W., Hunter, B.A., Wagner, J.L., Dabrowski, B., Vandervoort, K.G., Viswanathan, H.K. and Jorgensen, J.D. (1994) Structural and superconducting properties of $\text{La}_{2-x}\text{Sr}_x\text{CuO}_4$ as a function of Sr content, *Phys. Rev. B* **49**, 4163-4175.
2. Haskel, D., Stern, E.A., Dogan, F. and Moodenbaugh, A.R. (2000) XAFS study of the low-temperature tetragonal phase of $\text{La}_{2-x}\text{Ba}_x\text{CuO}_4$: Disorder, stripes, and T_c suppression at $x = 0.125$, *Phys. Rev. B* **61**, 7055-7076.
3. Haskel, D., Stern, E.A., Hinks, D.G., Mitchell, A.W., Jorgensen, J.D. and Budnick, J.I. (1996) Dopant and Temperature induced structural phase transitions in $\text{La}_{2-x}\text{Sr}_x\text{CuO}_4$, *Phys. Rev. Lett.* **76**, 439-442.
4. Haskel, D., Polinger, V and Stern, E.A. (1999) Where do the doped holes go in $\text{La}_{2-x}\text{Sr}_x\text{CuO}_4$? A close look by XAFS *High Temperature Superconductivity, AIP Conference Proceedings* **483**, 241-246.
5. Haskel, D., Stern, E.A., Hinks, D.G., Mitchell, A.W. and Jorgensen, J.D. (1997) Altered Sr environment in $\text{La}_{2-x}\text{Sr}_x\text{CuO}_4$, *Phys. Rev. B.* **56**, R521-524.
6. Hammel, P.C., Statt, B.W., Martin, R.L., Chou, F.C., Johnston, D.C. and Cheong, S.W. (1998) Localized holes in superconducting lanthanum cuprate, *Phys. Rev. B.* **57**, R712-715.
7. Chen, C.T., Tjeng, L.H., Kwo, J., Kao, H.L., Rudolf, P., Sette, F. and Fleming, R.M. (1992) Out of plane orbital character of intrinsic and doped holes in $\text{La}_{2-x}\text{Sr}_x\text{CuO}_4$, *Phys. Rev. Lett.* **68**, 2543-2547.
8. Phillips, J.C. (1999) Dopant sites and structure in high T_c layered cuprates, *Philos. Mag. B.* **79**, 1477-1498; Phillips, J.C. (1997) Filamentary microstructure and linear temperature dependence of normal state transport in optimized high temperature superconductors, *Proc. Natl. Acad. Sci. USA* **94**, 12771-12775; Phillips, J.C. (1999) Is there an ideal phase diagram for high T_c superconductors?, *Philos. Mag. B.* **79**, 527-536
9. Hasselmann, N., Castro Neto, A.H., Morais Smith, C. and Dimashko, Y (1999) Striped Phase in the Presence of Disorder and Lattice Potentials, *Phys. Rev. Lett.* **82**, 2135-2138.